

Article

Formulating and Optimizing a Novel Biochar-Based Fertilizer for Simultaneous Slow-Release of Nitrogen and Immobilization of Cadmium

Lu Chen ¹, Qincheng Chen ¹, Pinhua Rao ², Lili Yan ², Alghashm Shakib ¹ and Guoqing Shen ^{1,*}

¹ School of Agriculture and Biology, Shanghai Jiao Tong University, 800 Dongchuan Road, Shanghai 200240, China; chenlu0001@sjtu.edu.cn (L.C.); chenqincheng@sjtu.edu.cn (Q.C.); shakibalghashm@gmail.com (A.S.)

² School of Chemistry and Chemical Engineering, Shanghai University of Engineering Science, Shanghai 201620, China; raopinhua@hotmail.com (P.R.); lily.502@163.com (L.Y.)

* Correspondence: gqsh@sjtu.edu.cn; Tel.: +86-21-342-061-43

Received: 28 June 2018; Accepted: 2 August 2018; Published: 3 August 2018



Abstract: This study aimed to develop and optimize a novel biochar-based fertilizer composed of rice husk biochar and urea–hydrogen peroxide (UHP), which can simultaneously slowly release nitrogen and immobilize cadmium (Cd). Response surface methodology (RSM) was adopted to optimize the fertilizer formulation with the lowest nitrogen release rate. Under the optimized conditions, the cumulative nitrogen release rate of the biochar-based fertilizer was 17.63%, which was significantly lower than that of ordinary fertilizer. Elementary analysis, scanning electron microscopy (SEM) images, and Fourier transform infrared (FTIR) spectroscopy proved that UHP attached to the porous structures of the biochar. The adsorption test showed that the adsorption of Cd onto biochar-based fertilizer quickly reached equilibrium with an equilibrium adsorbing quantity (Q_e) of $6.3279 \text{ mg}\cdot\text{g}^{-1}$ with an initial concentration of $10 \text{ mg}\cdot\text{L}^{-1}$. Compared to original biochar, the Cd immobilization ability of biochar-based fertilizer was significantly better. The adsorption of Cd on biochar-based fertilizer is mainly based on a monolayer adsorption behavior. Finally, improved crop growth was demonstrated by pot experiments, which showed a significant increase in the biomass of cabbage. The concept and findings presented in this study may be used as references in developing a novel biochar-based fertilizer for simultaneously enhancing crop yield and reducing environmental risk.

Keywords: biochar-based fertilizer; urea–hydrogen peroxide; slow-release; nitrogen; immobilization; cadmium

1. Introduction

Fertilizers play a vital role in enhancing crop yield. Many diverse fertilizers have been applied to soil [1]. However, the use of fertilizers has been labeled by environmentalists as a main source of water and soil environment pollutants. The main environmental impacts associated with fertilizer use have been linked to leaching and runoff of nutrients, especially nitrogen, which causes aquatic eutrophication. The extensive use of fertilizers may also decrease the pH and increase the availability of heavy metals in soil [2]. Typically, cadmium is a highly hazardous metal, which can be easily absorbed by plants with a high transfer coefficient and then assimilated by animals and humans [3]. For example, Huang et al. reported that applying large amounts of compound fertilizers constantly increased the available content of Cd in soils. Accordingly, Cd absorbed by plants also increased [4]. Considering the crop production and environmental risk, researchers and fertilizer producers have attempted to search for means to achieve newly defined goals of fertilizer use: improved fertilizer nutrient use efficiency and reduced bio-availability of heavy metals in soil or fertilizers [5].

Biochar is a carbon-enriched product obtained by heating biomass under low-oxygen or oxygen-free conditions [6]. Biochar possesses specific properties, such as a porous structure, a relatively large surface area, a large number of functional groups, and abundant mineral elements, that benefit the immobilization of heavy metals and loading of fertilizer nutrients in soil. For example, Yousaf et al. [7] demonstrated that biochar decreases the availability and uptake of Cd in wheat. Numerous researchers also proved that supplementing biochar can reduce the fertilizer loss to improve soil fertility. For instance, Kimetu [8] and Mizuta et al. [9] demonstrated that biochar, which contains many functional groups, strongly adsorbs various nutrient ions, including nitrate, ammonium, phosphate, and potassium ions, to load nutrients and reduce soil nitrogen nutrient loss.

However, biochar itself does not contain enough nutrients for crop growth. Asai et al. [10] found that grain yield decreased when only applying biochar due to the insufficient supply of nitrogen (N). Thus, supplementing biochar with certain fertilizers (for example urea) renders biochar materials more suitable for stimulating plant growth [11] and heavy metal adsorption [12]. Due to the agricultural and environmental advantages, biochar-based fertilizer has been receiving increasing attention [13]. Many researchers have observed that biochar-based fertilizers delay the release of nutrients in soil and display a slow-release effect [14–17]. Supplementing biochar-based fertilizer can adjust the soil pH, reduce the bulk density to improve soil ventilation and permeability, and increase the crop yield significantly [18–20]. However, the effectiveness of biochar-based fertilizer for simultaneously slowly releasing nitrogen and immobilizing heavy metals requires further investigation. In the present study, we attempted to use urea–hydrogen peroxide (H_2NCONH_2 H_2O_2 (UHP)) and biochar to prepare a novel biochar-based fertilizer that can slowly release nitrogen and immobilize Cd simultaneously. UHP is an oxygen–nitrogen fertilizer composed of a complex of urea with hydrogen peroxide (H_2O_2). In agriculture, UHP exhibits two properties: it delivers oxygen through hydrogen peroxide and supplies nitrogen for fertilizer by urea. Frankenberger [21] demonstrated that using UHP as a watering solution after flooding can improve the aeration of soil and crop growth.

Although biochar-based fertilizers have many potential advantages, their storage, transport, and application to soil remain challenging due to their irritation of human skin, eyes, and respiratory system [22]. Husk and Major [23] found that 25% of their applied biochar was lost during field spreading. Moreover, due to heavy rainfall events, 20–53% of biochar applied to the soil ran off [24]. Therefore, the development of suitable biochar-based fertilizer products that can provide a long-term supply of nutrients and with a minimal loss of biochar is necessary. From this point of view, pelletization can significantly alleviate the loss of biochar during application to soil and reduce the costs of transport and handling [25]. However, some influencing factors, such as water addition, mass ratio of fertilizer to biochar, and binder addition, affect pelletization [26]. Thus, optimization is required. The traditional single-factor optimization is time-consuming and entails several experiments for determining the optimal levels. This technique is also unreliable because of its exclusion of the interactive effects among the variables studied [27].

In the present study, a novel biochar-based fertilizer composed of biochar and UHP was investigated for the simultaneous slow-release of N and enhancing Cd adsorption. We hypothesized that (1) urea from UHP can be slow-released from optimized biochar-based fertilizer and further stimulate crop growth; (2) H_2O_2 from UHP could increase oxygen-containing functional groups on the surface of biochar-based fertilizers and thus enhance its ability to adsorb Cd. The Box–Behnken design (BBD) of the response surface methodology (RSM), an effective statistical and optimization technique [28], was adopted to study the influences of important operating parameters, including water addition, mass ratio of fertilizer to biochar, and kaolin addition, on the release rate of nitrogen. The physicochemical properties of optimal biochar-based fertilizer were characterized in detail. The Cd adsorption capacity of the optimal biochar-based fertilizer was assessed through an adsorption experiment. The effect on crop growth was also investigated using pot experiments.

2. Materials and Methods

2.1. Preparation Process of Biochar-Based Fertilizer

Biochar was prepared through slow pyrolysis of rice husks at 500 °C. The biochar was then placed in UHP solution for 24 h at room temperature. After the impregnation procedure, the biochar-based fertilizer samples were transferred in an electric thermostatic drying oven at 60 °C for 24 h. The biochar-based fertilizer was crushed and passed through 40-mesh (i.e., 425 µm mesh size) standard metal sieves. Certain amounts of biochar-based fertilizer and kaolin were mixed and placed in a disc pelletizer to begin pelletization. The rotating speed of the turntable was adjusted to 30 r·min⁻¹, and the tilt angle of the turntable was 45°. When the material was fully mixed, distilled water was sprayed onto the granulator with an atomizer. After being shaped, the granular biochar-based fertilizer was removed from the disc granulator, placed in an electric thermostatic drying oven, and dried at 40 °C.

2.2. Optimizing Parameters Using RSM

To optimize the preparation conditions for the biochar-based fertilizer, Design-Expert 8.0.6 (Stat-Ease Inc., Minneapolis, MN, USA) with RSM was used. The total outline included three factors: water addition, mass ratio of fertilizer to biochar, and kaolin addition, each of which was coded at three levels (−1, 0, and 1; Table 1). Equation (1) was created by using RSM to determine the relationship between experimental factors and the response surface.

$$Y = A_0 + \sum_{i=1}^n A_i X_i + \sum_{i=1}^n A_{ii} X_i^2 + \sum_{i,j=1(i \neq j)}^n A_{ij} X_i X_j + \varepsilon \quad (1)$$

where Y is the response value predicted by the model; A_0 , A_i , A_{ii} , and A_{ij} represent the constant term and coefficients of the linear, squared, and interaction terms, respectively; and ε is the residual associated with the experiments.

Table 1. Levels and codes of experimental factors on the Box–Behnken design.

Level	Experimental Factors		
	Water Addition X_1 (%)	Fertilizer-Biochar Mass Ratio X_2	Kaolin Addition X_3 (%)
−1	5	0.1	5
0	15	1	15
1	25	1.9	25

2.3. Leaching through a Sand Column Experiment

A leaching experiment was performed in a series of specially designed polyvinyl chloride (PVC) columns (Figure 1). In this study, to reasonably evaluate the slow-release property, inert quartz sand (Shanghai Tian Scientific Co., Ltd., Shanghai, China) was used to create a pure system for our leaching experiment [29–31]. PVC tubes with an inner diameter of 4 cm and a height of 30 cm were used. The bottom of the tubes were sealed with double layer 100-mesh gauze, and 20 cm of each PVC tube was loaded with quartz sand that was passed through 40-mesh standard metal sieves. Distilled water was used for leaching. After the solution became clear and transparent, 5 g of biochar-based fertilizer was added and covered with 5-cm-thick quartz sand. The intermittent leaching test was initiated. To simulate natural rainfall, distilled water (100 mL) was slowly added every 24 h. The leaching solution was collected using 250 mL conical flasks. The urea content in the leaching solution was determined by spectrophotometry with *P*-dimethylaminobenzaldehyd [32]. Each group was measured three times. Equation (2) was used to calculate the urea content in the leaching solution. V represents the volume of leaching solution and c represents the concentration of leachate.

$$M = V \times c \quad (2)$$

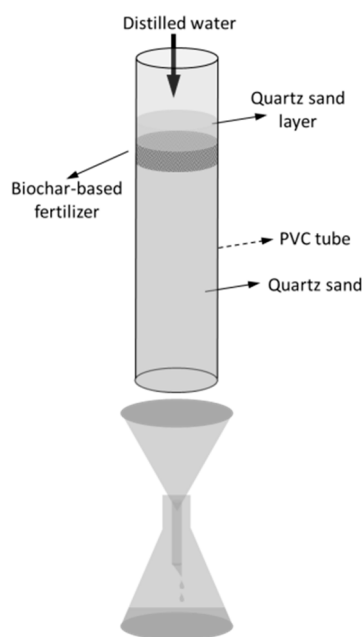


Figure 1. Overview of the column system.

2.4. Characterization of Biochar-Based Fertilizer

The concentrations of C, H, O, and N in biochar-based fertilizer were determined by an elemental analyzer (Vario EL Cube, Elementar, Langensfeld, Germany). The morphology of biochar-based fertilizer was analyzed by scanning electron microscopy (SEM). Fourier transform infrared (FTIR) spectroscopies of biochar-based fertilizer were characterized by a Nicolet 6700 spectrometer (Thermo Scientific, Waltham, MA, USA).

2.5. Adsorption Experiments

Adsorption experiments were conducted by mixing 0.5 g of biochar-based fertilizer with $10 \text{ mg}\cdot\text{L}^{-1}$ Cd^{2+} solution and stirring with a magnetic stirrer under 25°C . The samples were obtained at different times to determine the Cd^{2+} concentration by inductively coupled plasma optical emission spectrometry (ICP-OES). Equation (3) was used to calculate the equilibrium adsorption capacity:

$$Q_e = V(\rho_0 - \rho_e)/m \quad (3)$$

where V represents the volume (L) of Cd^{2+} solution; m represents the mass of biochar-based fertilizer (g); ρ_0 and ρ_e are the initial and final concentration ($\text{mg}\cdot\text{L}^{-1}$) of Cd^{2+} solutions, respectively; and Q_e represents the amount of Cd^{2+} adsorbed onto the biochar-based fertilizer ($\text{mg}\cdot\text{g}^{-1}$).

2.6. Pot Experiment Design

Three treatments, each with three replicates, were used in the current pot experiment: control, biochar, and biochar-based fertilizer treatment. A total of nine pots was used. These pots were placed in a greenhouse in a randomized arrangement. Each pot contained 300 g soil. The biochar and biochar-based fertilizer amendment rate was 2% w/w dry weight. Cabbage seeds (*Brassica chinensis* L.) were sprinkled on a filter paper moistened with deionized water in a petri dish. On day 7, germinated seeds were randomly chosen and replanted in soil with one plant per pot. All pots were watered every day under greenhouse conditions. After 30 days, all plant samples were harvested and weights of fresh biomass were determined.

3. Results and Discussion

3.1. Model Establishment and Analysis

Based on single-factor experiments, the effects of water addition (X_1), fertilizer–biochar mass ratio (X_2), and kaolin addition (X_3) on the slow-release ability of biochar-based fertilizer were determined by RSM. The corresponding ranges and cumulative release rate obtained from these ranges are listed in Table 2. The second-order polynomial model denoting the relationship between the response and the variables is as follows:

$$Y = 29.05 - 1.40X_1 + 3.94X_2 - 4.49X_3 + 0.55X_1X_2 + 1.31X_1X_3 + 1.19X_2X_3 + 1.54X_1^2 + 2.29X_2^2 - 4.62X_3^2. \quad (4)$$

Table 2. Experimental design and results of the cumulative release rate of urea ($n = 3$, $\sigma < 0.2$).

Runs	Code Factors			Response Y (%)	
	X_1	X_2	X_3	Actual	Predicted
1	0	1	−1	33.31	33.505
2	0	−1	−1	29.3	28.915
3	1	0	−1	27.95	27.75
4	−1	−1	0	31.35	31.345
5	1	0	1	21.77	21.380
6	1	1	0	35.51	35.515
7	0	−1	1	17.74	17.545
8	0	0	0	29.42	29.047
9	0	0	0	28.3	29.047
10	−1	0	1	21.37	21.570
11	0	0	0	29.42	29.047
12	−1	1	0	37.8	37.215
13	−1	0	−1	32.78	33.170
14	0	1	1	26.52	26.905
15	1	−1	0	26.85	27.435

Note: −1, 0, and 1 represent low, medium, and high levels, respectively; X_1 , water addition; X_2 , fertilizer–biochar ratio; X_3 , kaolin addition; and Y , cumulative release rate of urea.

Analysis of variance (ANOVA) was used to evaluate the significance of each factor and interaction terms. As shown in Table 3, the distinction between the coefficient of determination ($R^2 = 0.9944$) and adjusted coefficient of determination (Adjusted $R^2 = 0.9843$) was under 0.01. The model achieved a significant result, with a p value less than 0.001; the lack-of-fit p value ($p > 0.05$) verified that the model can adequately fit the experimental data. Figure 2a provides the plot of the predicted response versus actual response. Most of the points were scattered monotonously around the fitting line; this pattern indicates the good correlation between the predicted and actual responses. Figure 2b shows the residuals versus predicted responses. The residual points were scattered randomly; therefore, the obtained model can be adequate to describe the relationship between the cumulative release rate of urea and the factors.

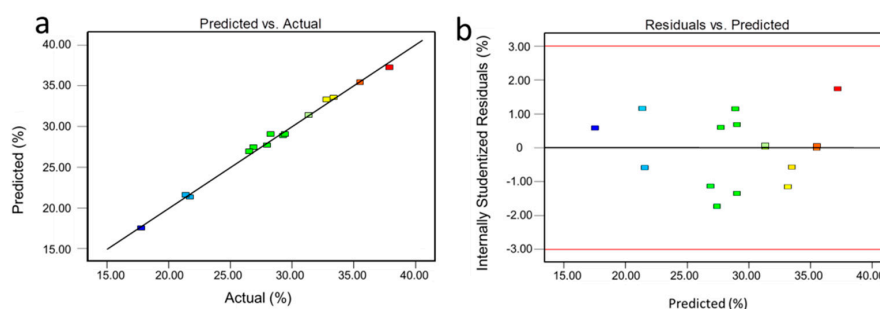


Figure 2. (a) Actual versus predicted cumulative release rate (%) of urea (correlation coefficient (R^2) = 0.9944, $n = 3$). (b) Residuals versus predicted cumulative release rate (%) of urea.

Table 3. ANOVA of the response surface quadratic model.

Source	Sum of Squares	Degrees of Freedom	Mean Square	F Value	p Value Prob > F
Model	403.92	9	44.88	98.53	<0.0001
X ₁ , water addition	15.74	1	15.74	34.55	0.0020
X ₂ , fertilizer–biochar ratio	97.30	1	97.30	213.62	<0.0001
X ₃ , kaolin addition	161.46	1	161.46	354.47	<0.0001
X ₁ X ₂	1.22	1	1.22	2.68	0.1625
X ₁ X ₃	6.84	1	6.84	15.01	0.0117
X ₂ X ₃	5.69	1	5.69	12.49	0.0167
X ₁ ²	8.76	1	8.76	19.24	0.0071
X ₂ ²	19.37	1	19.37	42.53	0.0013
X ₃ ²	78.80	1	78.80	172.99	<0.0001
Residual	2.28	5	0.46		
Lack of Fit	1.44	3	0.48	1.15	0.4966
Pure Error	0.84	2	0.42		
R ²			0.9944		
Adjusted R ²		0.9843			
Predicted R ²		0.9386			
Adequate Precision		35.695			

3.2. Effect of Interactive Variables

To illustrate the relationship between variables, we plotted response surface graphs (Figure 3). The relationship between water addition and fertilizer–biochar mass ratio is illustrated in Figure 3a. At a fixed fertilizer–biochar mass ratio (such as 1.9), the cumulative release rate decreased from 37.8 to 35.1% as water addition increased from 5 to 25%. This result was achieved because kaolin powder mixed with water molecules to produce a sticky material during agglomerate granulation. With increasing the particle size of biochar-based fertilizer, resistance was created when nutrients in particles migrated to the surface. Large fertilizer particle sizes resulted in a long nutrient transfer path from inside to outside, large resistance, and long travel time [33].

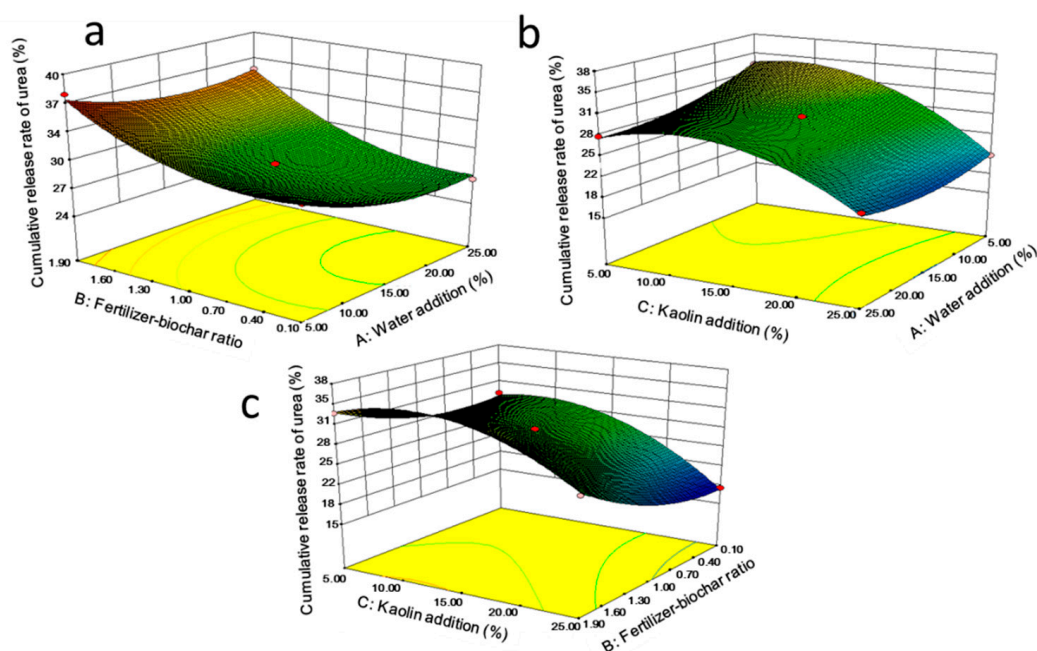


Figure 3. Response surfaces achieved using the Box–Behnken design: (a) water addition versus fertilizer–biochar rate, (b) water addition versus kaolin addition, and (c) fertilizer–biochar rate versus kaolin addition.

The fertilizer–biochar mass ratio exerted a negative effect on the cumulative release rate, meaning the response decreased as the biochar amount increased. This result is in accordance with Jiang's work [33]. The authors suggested that this effect was observed because some urea molecules entered the pores of the biochar given the dissolution by water, mechanical agitation, and biochar adsorption. The pores displayed a capillary effect due to their small pore size, and their strong adsorption of urea molecules enabled the biochar to release the urea slowly.

Figure 3b,c shows the response surface obtained by plotting kaolin addition versus water addition and fertilizer–biochar mass ratio. Kaolin addition exerted a negative effect on the cumulative release rate, with the response decreasing as the kaolin amount increased. This phenomenon occurred because higher kaolin amounts result in a high density of the fertilizer granules, which led to excellent resistance and a longer time for nutrients to migrate from inside to the particle surface [33].

3.3. Experimental Validation of the Optimized Conditions

We validated the optimized conditions for the lowest cumulative nitrogen release rate of biochar-based fertilizer. In particular, the optimized conditions for the slow-release ability of nitrogen from biochar-based fertilizer were observed at 16.89% water addition under the use of 25% kaolin when the fertilizer–biochar mass rate was 0.2. The minimum cumulative nitrogen release rate of the biochar-based fertilizer at this condition was 17.66%. The optimized conditions were validated repeatedly ($n = 3$). The results showed a cumulative nitrogen release rate of $17.63 \pm 0.004\%$. A good agreement between the experimental and calculated values (relative error = 0.178%) showed that biochar could be used successfully for slowing fertilizer release. Compared with the control (UHP application only, 68.66% of cumulative nitrogen release rate), application of biochar-based fertilizer reduced the overall cumulative nitrogen via leaching by 74.32%. Ding et al. [34] reported that application of bamboo charcoal reduced overall cumulative nitrogen via leaching by 15.2%. Therefore, the nitrogen slow-release in biochar-based fertilizer increased significantly. This may be ascribed to the H_2O_2 from UHP.

3.4. Characterization of Biochar-Based Fertilizer

The SEM images of the biochar and biochar-based fertilizers (Figure 4) depict the active porous structures on the biochar surface. Biochar (Figure 4a,b) exhibited a homogeneous pore distribution with a relatively clean and smooth pore surface. Comparatively, some wrinkles appeared on the pore surface of the biochar-based fertilizer sample, shown in Figure 4c,d. In addition, some white particles were adsorbed on the pore surface of the biochar-based fertilizer. This above phenomenon may indicate that the UHP fertilizers were strongly attached to the biochar without significantly influencing the pore structure.

Table 4 indicates that the total carbon contents in biochar and biochar-based fertilizer were 50.10% and 49.03%, respectively. The C/N ratio of biochar-based fertilizer was significantly lower compared with that of untreated biochar. This result implies that the N content in UHP was loaded onto the biochar and helped reduce the risk of effective nitrogen loss from soil, and thus the slow plant growth was due to the application of biochar only. The O/C ratio of biochar can reflect the stability of biological carbon in soil. Generally, a O/C ratio lower than 0.2 results in a minimum 1000 years of biochar half-life [35]. As shown in Table 4, the O/C ratios of biochar and biochar-based fertilizer were 0.17 and 0.18, respectively, which indicates that the rice-husk-derived biochar demonstrated good stability.

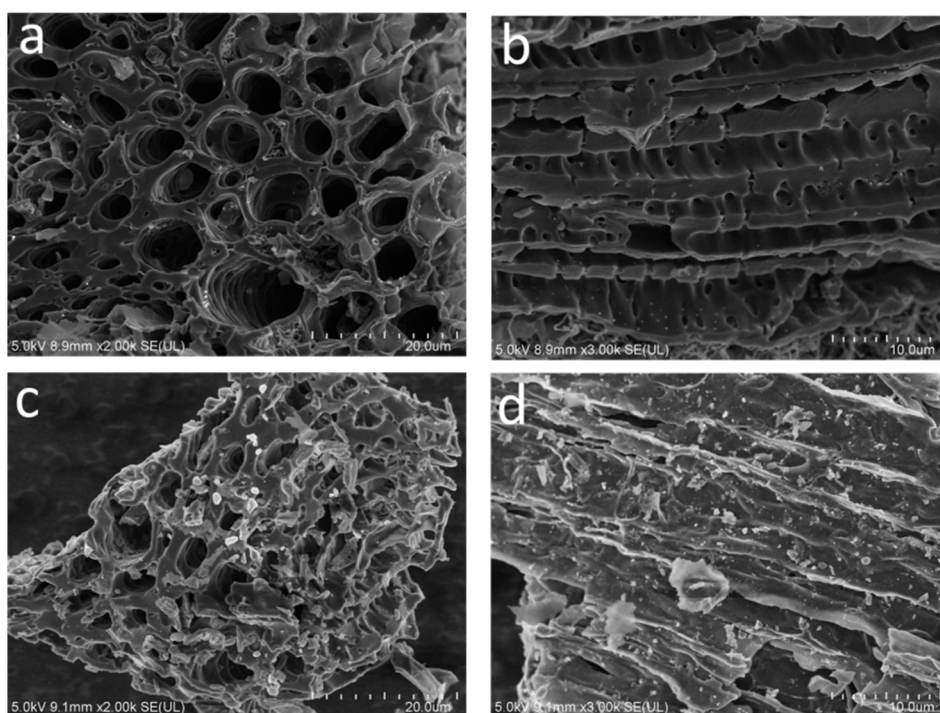


Figure 4. Scanning electron microscopy (SEM) micrographs of (a,b) biochar and (c,d) biochar-based fertilizer.

Table 4. Primary elements of biochar-based fertilizer, including the carbon–nitrogen (C/N) and oxygen–carbon (O/C) molar ratios.

Sample	C (%)	H (%)	N (%)	O (%)	C/N	O/C
Biochar	50.10	1.71	0.72	11.33	81.18	0.17
Biochar-based fertilizer	49.03	2.18	5.60	11.81	10.21	0.18

Fourier transform infrared (FTIR) spectroscopy is an established tool for detecting functional groups to further study adsorption behavior [36]. In this study, most of the FTIR spectra were similar for biochar and biochar-based fertilizer, except for the peak that appeared in biochar-based fertilizer at 1635 cm^{-1} corresponding to the stretching vibration of C=O (Figure 5) [37]. In addition, the broad peak at 2360 cm^{-1} , associated with the stretching vibration of C–O in biochar-based fertilizer, was stronger than that in biochar, implying the increase in C–O in biochar-based fertilizer [38]. The appearance of these oxygen-containing surface functional groups may be attributed to H_2O_2 from UHP, which can cause the oxidization of carbonized surfaces, thereby enhancing the biochar’s ability to adsorb heavy metals [39].

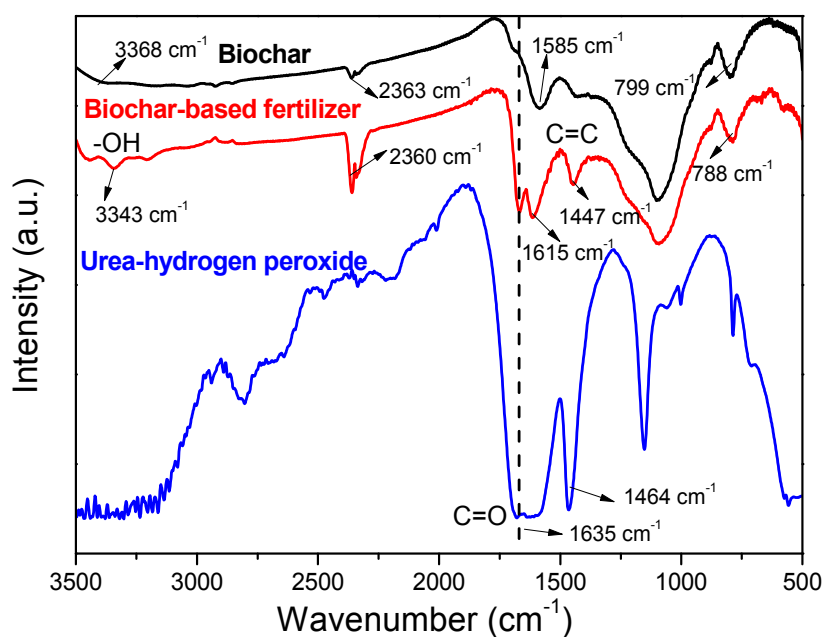


Figure 5. Stack plot of Fourier transform infrared (FTIR) spectra of biochar, biochar-based fertilizer, and urea–hydrogen peroxide (UHP).

3.5. Adsorption Kinetic Models for Cadmium

The adsorption kinetics are an important characteristic for defining the efficiency of adsorption [40]. Figure 6 shows the adsorption capacities of Cd^{2+} versus time at an initial concentration of $10 \text{ mg}\cdot\text{L}^{-1}$. At the initial stage of the adsorption process, the adsorption rate was very high. Then, the rate exhibited a gradual decrease until adsorption equilibrium was reached. From this characterization of the adsorption kinetics, the Cd^{2+} were initially rapidly adsorbed onto the exterior surface of biochar and then diffused into the pores of biochar and adsorbed onto their interior surface. Compared with the biochar, the time for biochar-based fertilizer to reach equilibrium decreased from 1400 min to 100 min, and the adsorption capacity increased from $4.2477 \text{ mg}\cdot\text{g}^{-1}$ to $5.9702 \text{ mg}\cdot\text{g}^{-1}$. Therefore, the amount of Cd^{2+} adsorbed onto the biochar-based fertilizer sample under equilibrium was larger than that of the biochar sample, indicating that the biochar-based fertilizer exhibited better Cd adsorption efficiency.

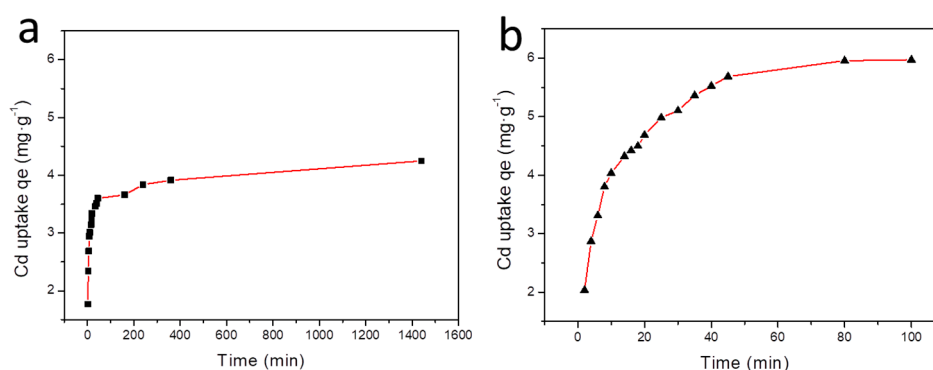


Figure 6. Adsorption kinetics of cadmium onto (a) biochar and (b) biochar-based fertilizer over time.

The adsorption kinetics of Cd on biochar and biochar-based fertilizer were analyzed by two well-known kinetic models: the pseudo-first-order model and the pseudo-second-order model, which are shown in Equations (5) and (6), respectively.

$$Q_t = Q_e(1 - \exp(-k_1t)) \quad (5)$$

$$Q_t = Q_e k_2 t / (1 + Q_m k_2 t) \quad (6)$$

where t denotes the contact time (min); Q_e and Q_t denote the amounts of Cd^{2+} ($\text{mg}\cdot\text{g}^{-1}$) adsorbed at equilibrium and a given time, respectively; and k_1 (min^{-1}) and k_2 ($\text{g}\cdot(\text{mg}\cdot\text{min})^{-1}$), calculated from the plots in Figure 7, are the rate constant of pseudo-first-order and pseudo-second-order kinetics, respectively. Accordingly, the R^2 value revealed that the correlation coefficient of the pseudo-second-order kinetic model was higher than that of the pseudo-first order kinetic model, which suggested that the kinetics of Cd^{2+} adsorption on biochar-based fertilizer could be described better by the pseudo-second-order equation. Figure 7 shows that the Cd sorption capacity of the biochar-based fertilizer significantly increased (48.98%) compared with that of biochar. When the initial concentration of Cd^{2+} was $10 \text{ mg}\cdot\text{L}^{-1}$, the adsorbing quantity at equilibrium of Cd on biochar-based fertilizer ($Q_e = 6.3279 \text{ mg}\cdot\text{g}^{-1}$) was higher than that on biochar ($Q_e = 4.2474 \text{ mg}\cdot\text{g}^{-1}$). Bhatnagar et al. [41] reported that the adsorption of cadmium significantly improved when carbon was oxidized, which was attributed to the generated carboxylic acid groups contributing to the adsorption of cadmium. Based on the above analysis and FTIR results, the increase in Cd adsorption capacity in our study may have been due to the oxygen-containing surface groups (Figure 5) on the biochar-based fertilizer.

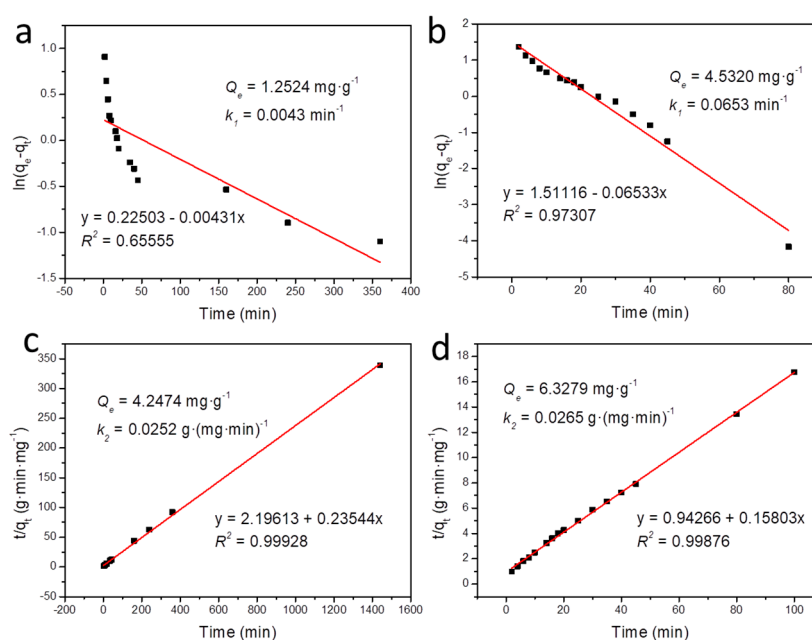


Figure 7. Kinetic models of Cd^{2+} adsorption onto the (a,c) biochar and (b,d) biochar-based fertilizer over time. (a,b) Pseudo-first-order plot and (c,d) pseudo-second-order plot.

3.6. Adsorption Isotherms

The typical adsorption isotherms of Cd on biochar and biochar-based fertilizer were investigated at initial concentrations ranging from 1 to $50 \text{ mg}\cdot\text{L}^{-1}$. As shown in Figure 8a, both for biochar and biochar-based fertilizer, the Cd^{2+} adsorption amounts gradually increased with the increase in Cd concentration. The amounts adsorbed on biochar-based fertilizer were higher than biochar. The obtained isotherm data were fitted and described using the Langmuir model and the Freundlich model, which are shown in Figure 8b,c, respectively. According to the obtained correlation coefficients,

the Langmuir model ($R^2 = 0.97884$ and 0.98146 for biochar and biochar-based fertilizer, respectively) can be used to fit the adsorption data better than the Freundlich model ($R^2 = 0.86798$ and 0.96117 for biochar and biochar-based fertilizer, respectively). These results indicated that the adsorption of Cd on biochar and biochar-based fertilizer is mainly based on a monolayer adsorption behavior.

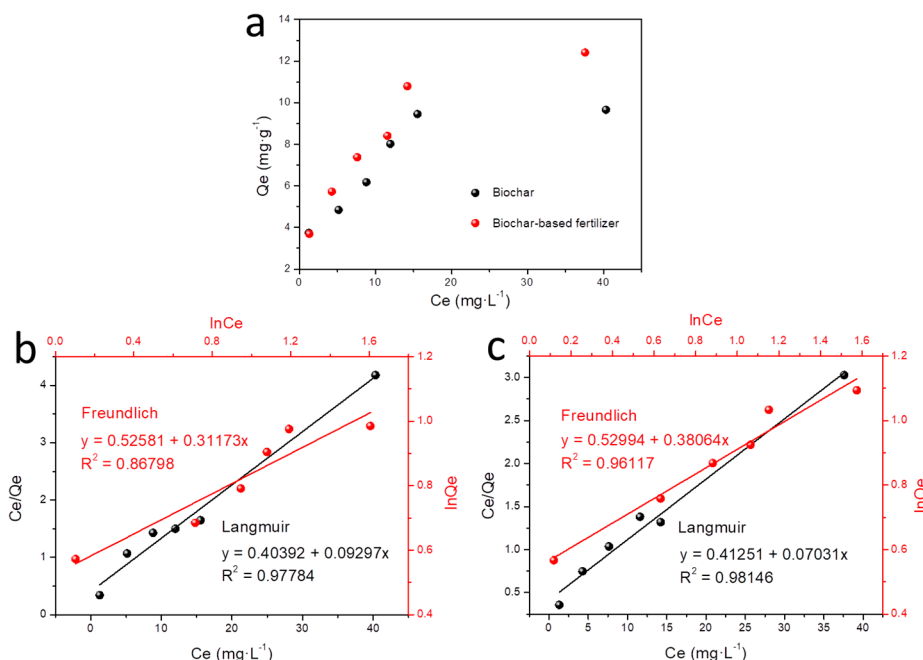


Figure 8. (a) Adsorption isotherm, the fitting Langmuir model (black), and the Freundlich model (red) for the Cd adsorption by (b) biochar and (c) biochar-based fertilizer.

3.7. Effects of Biochar-Based Fertilizer on Plant Growth

The improved crop growth was demonstrated using pot experiments. Figure 9a shows that the growth of *Brassica chinensis* L. in the pots with biochar-based fertilizer was much stronger and the foliage was greener than in the control and biochar treatments. The plants in biochar-based fertilizer possessed broader leaf blades, and the color of the foliage was darker green. Data on biomass, shown in Figure 9b, revealed that biochar-based fertilizer addition increased above-ground biomass by 83.58% over the unamended control (CK) and 87.79% over the biochar treatment. This finding indicated that the resulting biochar-based fertilizer has potential for improving fertilizer efficiency. Biochar has been shown to improve crop productivity in some but not all circumstances. In this study, biochar amendment had no significant improvement on cabbage growth. However, the below-ground biomass in the biochar-only treatment was 1.5–1.6 times higher than that in other treatments. A positive effect of biochar on root growth was also observed in pot experiments [42]. The root stimulation effect observed in these studies has frequently been ascribed to the changes in the soil physicochemical properties, such as pH and bulk density, that biochar could have induced. Ventura et al. [43] postulated a stimulating effect of biochar-derived organic compounds on plant root growth. Further studies concerning the mechanisms of biochar–UHP biochar-based fertilizer on plant growth and field-scale experiments should be conducted.

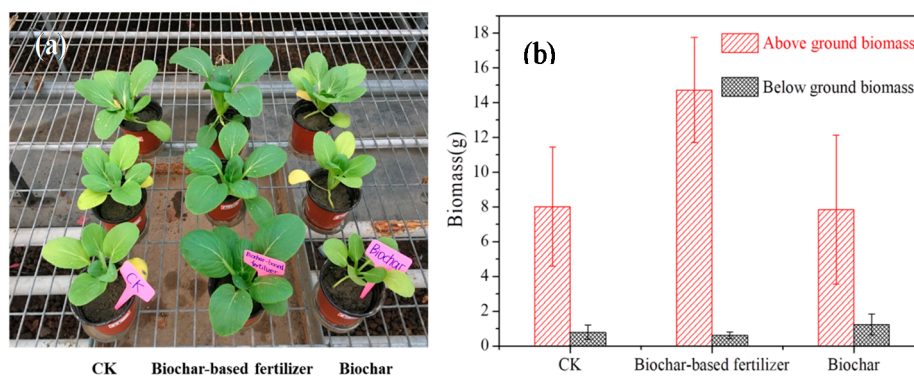


Figure 9. Photograph (a) and Biomass (b) of cabbage (*Brassica chinensis* L.) under different treatments. CK, unamended control.

4. Conclusions

In summary, in this work we prepared a novel biochar-based fertilizer (blended with fertilizer UHP followed by pelletization) that can simultaneously slowly release nitrogen and immobilize Cd. The optimized formulation for biochar-based fertilizer was obtained using RSM. The minimum cumulative release rate of granular biochar-based fertilizer was 17.63%, which was obtained through a leaching experiment in an inert quartz sand system. The observed response was close to the predicted value for the optimized formulation (17.66%). Morphology and component characterization showed that UHP attached onto the porous surface of the biochar, leading to a novel biochar-based fertilizer. The Cd adsorption onto biochar-based fertilizer reached equilibrium, with an equilibrium adsorbing quantity of $6.3279 \text{ mg} \cdot \text{g}^{-1}$ following the pseudo-second-order model with the initial concentration of Cd ($10 \text{ mg} \cdot \text{L}^{-1}$). The adsorption capacity of biochar-based fertilizer toward Cd increased significantly by 48.98% compared to that of biochar. The results from adsorption isotherms indicated that the adsorption of Cd on biochar and biochar-based fertilizer is mainly based on a monolayer adsorption behavior. The pot experiments showed that the resulting granular biochar-based fertilizer is beneficial for the growth of cabbage. We think that the results in our work are of significance for the design and development of a novel biochar-based fertilizer with high crop yield and low environmental risk.

Author Contributions: Conceived and designed the paper: G.S. and L.C. Collected and analyzed data: L.C., Q.C., and P.R. Wrote the paper: G.S., L.C., L.Y., and A.S.

Funding: This research was funded by the National Key Research and Development Program of China (No. 2018YFD0800205), the SUES Sino-foreign Cooperative Innovation center for City Soil Ecological Technology Integration (2017PT03) and First-rate Discipline Construction of Applied Chemistry of Shanghai University of Engineering Science (No. 2018xk-B-06).

Conflicts of Interest: The authors declare no conflict of interest.

References

1. Qiao, D.L.; Liu, H.S.; Yu, L.; Bao, X.Y.; Simon, G.P.; Petinakis, E.; Chen, L. Preparation and characterization of slow-release fertilizer encapsulated by starch-based superabsorbent polymer. *Carbohydr. Polym.* **2016**, *147*, 146–1541. [[CrossRef](#)] [[PubMed](#)]
2. Haygarth, P.M.; Jarvis, S.C. *Agriculture, Hydrology and Water Quality*, 1st ed.; CABI Publishing: Oxford, NY, USA, 2002; ISBN 0-85199-545-4.
3. Qi, F.J.; Dong, Z.M.; Lamb, D.; Naidu, R.; Bolan, N.S.; Ok, Y.S.; Liu, C.; Khan, N.; Johir, M.A.H.; Semple, K.T. Effects of acidic and neutral biochars on properties and cadmium retention of soils. *Chemosphere* **2017**, *180*, 564–573. [[CrossRef](#)] [[PubMed](#)]
4. Huang, B.; Kuo, S.; Bembenek, R. Availability of cadmium in some phosphorus fertilizers to field-grown lattuc. *Water Air Soil Pollut.* **2004**, *158*, 37–51. [[CrossRef](#)]

5. Su, C.; Jiang, L.Q.; Zhang, W.J. A review on heavy metal contamination in the soil worldwide: Situation, impact and remediation techniques. *Environ. Scept. Critics* **2014**, *3*, 24–38.
6. Sohi, S.P. Carbon storage with benefits. *Science* **2012**, *338*, 1034–1035. [[CrossRef](#)] [[PubMed](#)]
7. Yousaf, B.; Liu, G.J.; Wang, R.W.; Rehman, M.Z.; Rizwan, M.S.; Imtiaz, M.; Murtaza, G.; Shakoor, A. Investigating the potential influence of biochar and traditional organic amendments on the bioavailability and transfer of Cd in the soil-plant system. *Environ. Earth Sci.* **2016**, *75*, 374. [[CrossRef](#)]
8. Kimetu, J.M.; Lehmann, J. Stability and stabilisation of biochar and green manure in soil with different organic carbon contents. *Aust. J. Soil Res.* **2010**, *48*, 577–585. [[CrossRef](#)]
9. Mizuta, K.; Matsumoto, T.; Hatate, Y.; Nishihara, K.; Nakanishi, T. Removal of nitrate nitrogen from drinking water using bamboo powder charcoal. *Bioresour. Technol.* **2004**, *95*, 255–257. [[CrossRef](#)] [[PubMed](#)]
10. Asai, H.; Samson, B.K.; Stephan, H.M.; Songyikhangsuthor, K.; Homma, K.; Kiyono, Y.; Inoue, Y.; Shiraiwa, T.; Horie, T. Biochar amendment techniques for upland rice production in Northern Laos: 1. Soil physical properties, leaf SPAD and grain yield. *Field Crop. Res.* **2009**, *111*, 81–84. [[CrossRef](#)]
11. Si, L.; Xie, Y.; Ma, Q.; Wu, L. The Short-Term Effects of Rice Straw Biochar, Nitrogen and Phosphorus Fertilizer on Rice Yield and Soil Properties in a Cold Waterlogged Paddy Field. *Sustainability* **2018**, *10*, 537. [[CrossRef](#)]
12. Zhao, L.; Cao, X.; Zheng, W.; Scott, J.W.; Sharma, B.K.; Chen, X. Copyrolysis of Biomass with Phosphate Fertilizers to Improve Biochar Carbon Retention, Slow Nutrient Release, and Stabilize Heavy Metals in Soil. *ACS Sustain. Chem. Eng.* **2016**, *4*, 1630–1636. [[CrossRef](#)]
13. Chen, P.; Sun, M.X.; Zhu, Z.X.; Zhang, J.D.; Shen, G.Q. Optimization of ultrasonic-assisted extraction for determination of polycyclic aromatic hydrocarbons in biochar-based fertilizer by gas chromatography-mass spectrometry. *Anal. Bioanal. Chem.* **2015**, *407*, 6149–6157. [[CrossRef](#)]
14. Khan, M.A.; Kim, K.K.; Wang, M.Z.; Lim, B.K.; Lee, W.H.; Lee, J.Y. Nutrient-impregnated charcoal: An environmentally friendly slow-release fertilizer. *Environmentalist* **2008**, *28*, 231–235. [[CrossRef](#)]
15. Lee, J.W.; Hawkins, B.; Li, X.N.; Day, D.M. Biochar fertilizer for soil amendment and carbon sequestration. In *Advanced Biofuels and Bioproducts*; Springer: New York, NY, USA, 2013; pp. 57–68.
16. Hagemann, N.; Kammann, C.I.; Schmidt, H.P.; Kappler, A.; Behrens, S. Nitrate capture and slow release in biochar amended compost and soil. *PLoS ONE* **2017**, *12*, e0171214. [[CrossRef](#)] [[PubMed](#)]
17. Day, D.; Evans, R.J.; Lee, J.W.; Reicosky, D. Valuable and stable carbon co-product from fossil fuel exhaust scrubbing. *Prepr. Pap. Am. Chem. Soc. Div. Fuel Chem.* **2004**, *49*, 352–355.
18. Agegnehu, G.; Bass, A.M.; Nelson, P.N.; Bird, M.I. Benefits of biochar, compost and biochar-compost for soil quality, maize yield and greenhouse gas emissions in a tropical agricultural soil. *Sci. Total Environ.* **2016**, *543*, 295–306. [[CrossRef](#)] [[PubMed](#)]
19. Gao, H.Y.; He, X.S.; Chen, X.X. Effect of biochar and biochar-based ammonium nitrate fertilizers on soil chemical properties and crop yield. *J. Agro-Environ. Sci.* **2012**, *31*, 1948–1955.
20. Li, Y.; Sun, Y.; Liao, S.; Zou, G.; Zhao, T.; Chen, Y.; Yang, J.; Zhang, L. Effects of two slow-release nitrogen fertilizers and irrigation on yield, quality, and water-fertilizer productivity of greenhouse tomato. *Agric. Water Manag.* **2017**, *186*, 139–146. [[CrossRef](#)]
21. Frankenberger, W.T. Factors Affecting the Fate of Urea Peroxide Added to Soil. *Bull. Environ. Contam. Toxicol.* **1997**, *59*, 50–57.
22. Schwab, C.V.; Hanna, H.M. *Master Gardeners' Safety Precautions for Handling, Applying, and Storing Biochar*; Agricultural and Biosystems Engineering Extension and Outreach Publications: Ames, IA, USA, 2012; p. 5.
23. Husk, B.; Major, J. *Commercial Scale Agricultural Biochar Field Trial in Québec, Canada over Two Years: Effects of Biochar on Soil Fertility, Biology and Crop Productivity and Quality*; Blue Leaf Inc.: Quebec, QC, Canada, 2010.
24. Major, J.; Lehmann, J.; Rondon, M.; Goodale, C. Fate of soil-applied black carbon: Downward migration, leaching and soil respiration. *Glob. Chang. Biol.* **2010**, *16*, 1366–1379. [[CrossRef](#)]
25. Reza, M.T.; Lynam, J.G.; Vasquez, V.R.; Coronella, C.J. Pelletization of biochar from hydrothermally carbonized wood. *Environ. Prog. Sustain. Energy* **2012**, *31*, 225–234. [[CrossRef](#)]
26. Chen, S.L.; Yang, M.; Ba, C.; Yu, S.S.; Jiang, Y.F.; Zou, H.T.; Zhang, Y. Preparation and characterization of slow-release fertilizer encapsulated by biochar-based waterborne copolymers. *Sci. Total Environ.* **2018**, *615*, 431–437. [[CrossRef](#)]
27. Bezerra, M.A.; Santelli, R.E.; Oliveira, E.P.; Villar, L.S.; Escalera, L.A. Response surface methodology (RSM) as a tool for optimization in analytical chemistry. *Talanta* **2008**, *76*, 965–977. [[CrossRef](#)] [[PubMed](#)]

28. Ge, Y.; Ge, M. Development of tea tree oil-loaded liposomal formulation using response surface methodology. *J. Liposome Res.* **2015**, *25*, 222–231. [[CrossRef](#)] [[PubMed](#)]
29. Perrin, T.S.; Boettinger, J.L.; Drost, D.T.; Norton, J.M. Decreasing Nitrogen Leaching from Sandy Soil with Ammonium-Loaded Clinoptilolite. *J. Environ. Qual.* **1998**, *27*, 656–663. [[CrossRef](#)]
30. Mukherjee, A.; Zimmerman, A.R. Organic carbon and nutrient release from a range of laboratory-produced biochars and biochar-soil mixtures. *Geoderma* **2012**, *193–194*, 122–130. [[CrossRef](#)]
31. Akinremi, O.O.; Cho, C.M. Phosphate and accompanying cation transport in a calcareous cation-exchange resin system. *Soil Sci. Soc. Am. J.* **1991**, *55*, 959–964. [[CrossRef](#)]
32. Hussain, I.; Mahmood, Z.; Yasmeen, R.; Jahangir, M.; Hammed, R.; Nasir, R. Assay of urea with p-dimethylaminobenzaldehyde. *J. Chem. Soc. Pak.* **2002**, *24*, 122–128.
33. Jiang, E.; Zhang, W.; Qing, L.; Wang, M.; Luo, L. Study on preparation of granular biochar-based urea and property. *J. Northeast Agric. Univ.* **2014**, *45*, 89–94.
34. Ding, Y.; Liu, Y.X.; Wu, W.X.; Shi, D.Z.; Yang, M.; Zhong, Z.K. Evaluation of biochar effects on nitrogen retention and leaching in multi-layered soil columns. *Water Air Soil Pollut.* **2010**, *213*, 47–55. [[CrossRef](#)]
35. Spokas, K.A. Review of the stability of biochar in soils: Predictability of O: C molar ratios. *Carbon Manag.* **2010**, *1*, 289–303. [[CrossRef](#)]
36. Yenisoy-Karakaş, S.; Aygün, A.; Güneş, M.; Tahtasakal, E. Physical and chemical characteristics of polymer-based spherical activated carbon and its ability to adsorb organics. *Carbon* **2004**, *42*, 477–484. [[CrossRef](#)]
37. Byler, D.M.; Susi, H. Examination of the secondary structure of proteins by deconvolved FTIR spectra. *Biopolymers* **1986**, *25*, 469–487. [[CrossRef](#)] [[PubMed](#)]
38. Liu, P.; Jiang, R.; Zhou, W.; Zhu, H.; Xiao, W.; Wang, D.; Mao, X. g-C₃N₄ Modified biochar as an adsorptive and photocatalytic material for decontamination of aqueous organic pollutants. *Appl. Surf. Sci.* **2015**, *358*, 231–239.
39. Song, X.L.; Liu, H.Y.; Cheng, L.; Qu, Y.X. Surface modification of coconut-based activated carbon by liquid-phase oxidation and its effects on lead ion adsorption. *Desalination* **2010**, *255*, 78–83. [[CrossRef](#)]
40. Kılıç, M.; Kırbıyık, C.; Çepelioğullar, Ö.; Pütün, A.E. Adsorption of heavy metal ions from aqueous solutions by bio-char, a by-product of pyrolysis. *Appl. Surf. Sci.* **2013**, *283*, 856–862. [[CrossRef](#)]
41. Bhatnagar, A.; Hogland, W.; Marques, M.; Sillanpää, M. An overview of the modification methods of activated carbon for its water treatment applications. *Chem. Eng. J.* **2013**, *219*, 499–511. [[CrossRef](#)]
42. Prendergast-Miller, M.T.; Duvall, M.; Sohi, S.P. Localisation of nitrate in the rhizosphere of biochar-amended soils. *Soil Biol. Biochem.* **2011**, *43*, 2243–2246. [[CrossRef](#)]
43. Ventura, M.; Zhang, C.; Baldi, E.; Fornasier, F.; Sorrenti, G.; Panzacchi, P.; Tonon, G. Effect of biochar addition on soil respiration partitioning and root dynamics in an apple orchard. *Eur. J. Soil Sci.* **2014**, *65*, 186–195. [[CrossRef](#)]

